Identification and Validation of the Mitochondrial F₁F₀-ATPase as the Molecular Target of the Immunomodulatory Benzodiazepine Bz-423

Kathryn M. Johnson,[1,2] Xueni Chen,[1]
Anthony Boitano,[1] Lara Swenson,[1]
Anthony W. Opipari, Jr.,[3,*] and Gary D. Glick[1,2,*]
[1]Department of Chemistry
[2]Graduate Program in Immunology
[3]Department of Obstetrics and Gynecology
University of Michigan
Ann Arbor, Michigan 48109

Summary

Bz-423 is a 1,4-benzodiazepine that suppresses disease in lupus-prone mice by selectively killing pathogenic lymphocytes, and it is less toxic compared to current lupus drugs. Cells exposed to Bz-423 rapidly generate O_2^- within mitochondria, and this reactive oxygen species is the signal initiating apoptosis. Phage display screening revealed that Bz-423 binds to the oligomycin sensitivity conferring protein (OSCP) component of the mitochondrial F_1F_0-ATPase. Bz-423 inhibited the F_1F_0-ATPase in vitro, and reconstitution experiments demonstrated that inhibition was mediated by the OSCP. This target was further validated by generating cells with reduced OSCP expression using RNA interference and studying the sensitivity of these cells to Bz-423. Our findings help explain the efficacy and selectivity of Bz-423 for autoimmune lymphocytes and highlight the OSCP as a target to guide the development of novel lupus therapeutics.

Introduction

The autoimmune disorder systemic lupus erythematosus (SLE) afflicts up to 1,000,000 Americans [1]. The central immunologic disturbance of SLE is the loss of B and T cell peripheral tolerance [2], and the resulting pathology is characterized by nonspecific inflammation in a variety of tissues and organs, including the kidney, where immune complex deposition and abnormal cellular proliferation can lead to renal failure [3]. The cause of SLE is unknown, and disease susceptibility appears to be influenced by multiple genes and environmental factors [4]. Currently, SLE treatment is empirical and employs anti-inflammatories, antimetabolites, and immunosuppressives that affect both pathogenic and normal cells [5, 6]. While patient survival has improved over the past 50 years, the morbidity from both the disease and therapy remains significant. Agents that act more specifically against lupus-determining lymphoid cells would represent a key advance in the treatment of SLE and related autoimmune disorders.

A principal difficulty in developing new therapies for SLE is the lack of cogent molecular targets for pharmacological intervention [5]. Autoreactive lymphocytes compose only a small percentage of the total lymphocyte repertoire in SLE, and the molecular basis for their autoreactivity and pathogenicity is largely unknown [2]. In the absence of molecular targets, diversity-oriented synthesis coupled to phenotype screening is a powerful method for identifying new, biologically active compounds [7]. Using this approach, we recently discovered a 1,4-benzodiazepine (Bz-423, Figure 1A) that induces apoptosis in lymphoid cells. When administered to lupus-prone autoimmune (NZB × NZW)F₁ (NZB/W) [8] and MRL/*MpJ-Fas^lpr* (MRL-*lpr*) mice [9], Bz-423 specifically induced apoptosis in pathogenic lymphocytes, attenuated disease progression, and prolonged survival. In NZB/W mice, activated germinal center (GC) B cells were killed, whereas activated splenic CD4⁺ T cells were targeted in the MRL-*lpr* strain. Unlike current anti-lupus drugs, the therapeutic dosage of Bz-423 suppressed autoimmune disease without adverse toxicity or suppression of normal immune function.

Subcellular fractionation studies revealed that Bz-423 acts directly on mitochondria, rapidly inducing superoxide (O_2^-) from the mitochondrial respiratory chain (MRC) [8]. This reactive oxygen species (ROS) functions as the key signal to initiate the permeability transition (PT), cytochrome *c* release, and apoptosis. These conclusions were based on experiments showing that: Bz-423 produced a dose-dependent increase in O_2^-; the amount of apoptosis produced by a given [Bz-423] is directly proportional to the amount of O_2^- induced; and antioxidants like vitamin E or the manganese superoxide dismutase mimetic, manganese(III)*meso*-tetrakis(4-benzoic acid)porphyrin (MnTBAP), blocked all downstream events leading to and including cell death [8]. The O_2^- response only occurred within coupled, actively respiring mitochondria (i.e., state 3), which is characteristic of F_1F_0-ATPase inhibitors [10]. Blocking the activity of this enzyme during active respiration places mitochondria in state 4 (a resting state), which leaves the MRC in a reduced form that favors reduction of O_2 to O_2^- at MRC complex III. Importantly, the O_2^- response was also observed in the lymphoid tissue of mice dosed with Bz-423, linking this mechanism to the therapeutic response [8].

Based on the properties of Bz-423 and its therapeutic potential, a series of experiments was conducted to identify and characterize its subcellular target. We find that Bz-423 inhibits the mitochondrial F_1F_0-ATPase both in isolated mitochondrial preparations and in whole cells, and inhibition is mediated by the oligomycin sensitivity conferring protein (OSCP) subunit of the enzyme, a component for which limited structural, biochemical, and mechanistic information is available [11]. Recent studies suggest that lupus lymphocytes have increased numbers of mitochondria, and these mitochondria have altered bioenergetic and redox properties that would sensitize them to an F_1F_0-ATPase inhibitor like Bz-423 [12–14]. Collectively, these studies validate the mitochondrial F_1F_0-ATPase as a drug target

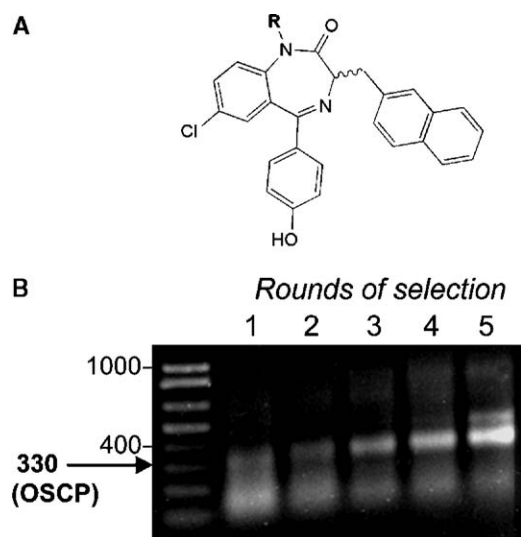*Correspondence: aopipari@umich.edu (A.W.O.); gglick@umich.edu (G.D.G.)

A

B

Rounds of selection

1 2 3 4 5

1000—

400—

330 →
(OSCP)

Figure 1. Structure and Target of Bz-423

(A) Chemical structure of Bz-423 (R = CH$_3$) and Bz-423-biotin conjugate [R = (CH$_2$)$_6$NH-biotin]. Bz-423 does not bind to GABA receptors and therefore is not anxiolytic, and binding to the peripheral benzodiazepine receptor (PBR) is weak (K$_d$ > 1 μM). The biotin linker does not alter the cytotoxic activity of Bz-423.

(B) Phage display selects the OSCP. Semiquantitative PCR using primers specific for the OSCP sequence reveals enrichment of clones encoding the OSCP with each round of selection using immobilized Bz-423. The cloned fragment represents 85% of the full-length protein.

for SLE and suggest that molecules like Bz-423 are promising leads.

Results

Bz-423 Binds to the OSCP and Inhibits the Mitochondrial F$_1$F$_0$-ATPase In Vitro

Previous studies demonstrated that Bz-423-induced mitochondrial O$_2^-$ is the second messenger initiating apoptosis in response to this agent, which suggested that a mitochondrial redox enzyme might be the molecular target of Bz-423. However, treating cells with inhibitors of the MRC enzymes or inhibitors of other redox proteins did not block the action of Bz-423, arguing against this hypothesis. Next, we investigated the involvement of >40 upstream molecular targets that could trigger proapoptotic signaling pathways in lymphocytes using both whole cell and in vitro screens (e.g., kinases; phosphatases; H$^+$, K$^+$/Na$^+$, and Ca^{2+}-ATPases; ion transporters; ion channels; redox enzymes; death receptors; caspases; Bcl-2 family members; and components of the permeability transition (PT) pore). These studies failed to identify the target of Bz-423 responsible for apoptosis.

As an alternative approach, an immobilized biotinylated analog of Bz-423 was used to screen a human cDNA T7 phage display library for the target [15]. After five successive rounds of selection and amplification, 20 phage clones were randomly selected and their inserts sequenced. Nine unique sequences were obtained, four of which had database matches. Only one of these clones contained a cDNA that was in-frame

with the C10 phage coat protein—this cDNA contained the coding region for amino acids 27–202 of the OSCP (Figure 1B).

The OSCP is part of a peripheral stalk that links the integral membrane F$_0$ component of the mitochondrial F$_1$F$_0$-ATPase with its soluble catalytic F$_1$ domain [16]. This 213 amino acid long protein (including the 23 amino acid mitochondrial leader sequence) is highly conserved among mammals and is not present in other ATPases. To determine if Bz-423 affected the enzymatic activity of the F$_1$F$_0$-ATPase, submitochondrial particles (SMPs) were prepared from bovine heart and treated with Bz-423, and F$_1$F$_0$-ATPase activity was evaluated. Bz-423 inhibited both the synthetic and hydrolytic activities of this enzyme (Figure 2A). Neither PK11195, a benzodiazepine analog that binds tightly to the peripheral benzodiazepine receptor (PBR) [17], nor diazepam, which binds γ-aminobutyric acid (GABA) receptors in the central nervous system, had any effect, demonstrating that the ability of Bz-423 to inhibit the F$_1$F$_0$-ATPase distinguishes it from other known benzodiazepines. F$_1$F$_0$-ATPase inhibition kinetics revealed that Bz-423 affects both V$_{max}$ and K$_m$, whereas oligomycin, which blocks proton transport in F$_0$ [18], affects only V$_{max}$ (Figure 2B). These data demonstrate that the mechanisms by which these compounds inhibit the enzyme are different; while the full implications of these differences are still being explored, they predict that F$_1$F$_0$-ATPase inhibition by Bz-423 and oligomycin will have different consequences in vivo.

To determine whether the OSCP was required for Bz-423-mediated F$_1$F$_0$-ATPase inhibition, we purified and reconstituted different portions of the ATPase, with and without the OSCP. F$_1$ can be solubilized away from F$_0$ and the peripheral stalk and retain its hydrolytic (but not synthetic) function [19]. F$_0$ can be obtained by sequentially depleting SMPs of the inhibitor protein (IF1), F$_1$, and the OSCP, yielding ΔSMPs [20]. Purified F$_1$ can then be reconstituted with recombinant OSCP alone (F$_1$•OSCP), ΔSMPs alone (F$_1$•ΔSMPs), or OSCP and ΔSMPs (F$_1$•OSCP•ΔSMPs) [21]. If the OSCP was required for inhibition, enzyme preparations lacking the OSCP should be insensitive to Bz-423.

Bz-423 inhibited the hydrolytic activity of purified F$_1$•OSCP complexes and F$_1$•OSCP•ΔSMPs (Figure 3A). In contrast, Bz-423 did not significantly inhibit ATP hydrolysis by purified F$_1$ and had a small effect (ca. 30%) on F$_1$•ΔSMPs, which likely resulted from the residual OSCP still present in the ΔSMPs (Figure 3B, lane 4; it is not possible to fully remove the OSCP through biochemical depletion [20]). This conclusion is further supported by the fact that oligomycin, which requires the OSCP to inhibit hydrolysis, inhibited F$_1$•ΔSMPs to a degree identical to that seen with Bz-423 (10 μM). The OSCP makes contacts with both F$_0$ and F$_1$, and it binds F$_1$•ΔSMPs much more tightly than F$_1$ alone [22]. Therefore, the difference in the potency of Bz-423 against F$_1$•OSCP versus F$_1$•OSCP•ΔSMPs probably reflects the reduced stability of the F$_1$•OSCP complex.

Bz-423 Inhibits the Mitochondrial F$_1$F$_0$-ATPase in Cells

A series of experiments was performed to determine if the effects of Bz-423 on living cells were consistent
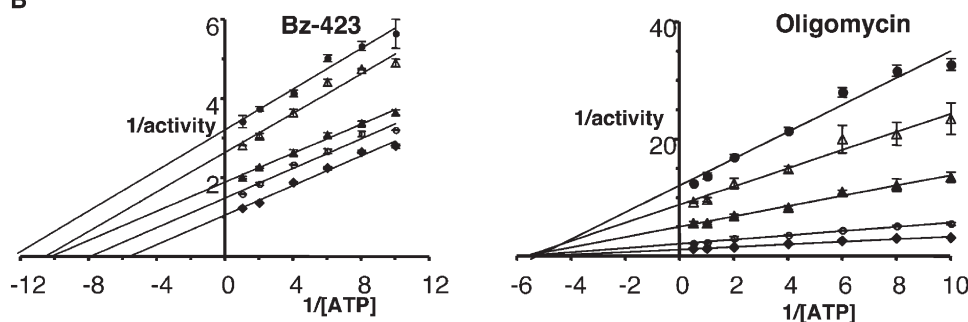
A
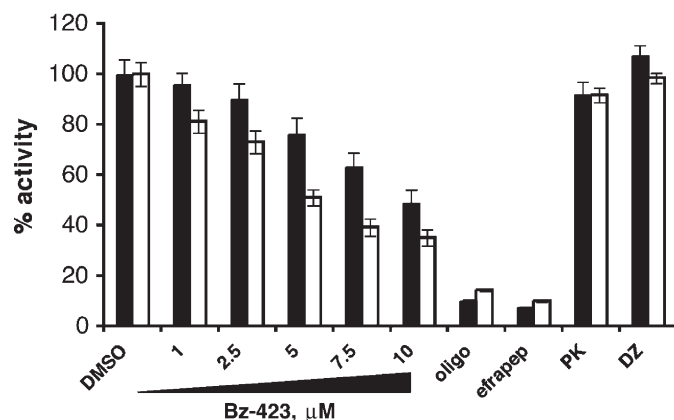
B

Figure 2. Bz-423 Inhibits the F_1F_o-ATPase

(A) Bovine SMPs were treated with Bz-423, and rates of ATP synthesis (filled bars) and hydrolysis (open bars) were determined using NADP$^+$ and NADH-coupled assays, respectively. Oligomycin (oligo; 0.1 μM) and efrapeptin (efrapep; 1 μM) are known F_1F_o-ATPase inhibitors. PK = PK11195 (10 μM); and DZ = diazepam (10 μM). The ATP synthesis and hydrolysis activities of the SMPs were 0.2 and 0.9 μmol/min/mg protein, respectively, in the absence of inhibitors. None of the inhibitors affected the activity of the coupling enzymes used in either assay.

(B) Double reciprocal plot of ATP hydrolysis activity in SMPs. Inhibition by Bz-423 (left; vehicle control [closed diamonds]; Bz-423: 5 [open circles], 7.5 [closed triangles], 10 [open triangles], 15 [closed circles] μM) compared to oligomycin (right; control [closed diamonds]; oligomycin: 10 nM [open circles], 25 nM [closed triangles], 50 nM [open triangles], 100 nM [closed circles]).

Error bars represent the standard deviation from at least three separate determinations.

with inhibition of the F_1F_0-ATPase. Because inhibition of the F_1F_0-ATPase prevents proton flow from the inter-membrane space back into the mitochondrial matrix [23], F_1F_0-ATPase inhibitors hyperpolarize the mitochondrial membrane potential (MMP) [24]. Thus, we sought to examine the effect of Bz-423 on the MMP in Ramos cells, a Burkitt's lymphoma cell line with a GC phenotype [25] in which most of the mechanistic data on Bz-423 has been obtained [8, 26]. MMP was monitored using the potentiometric fluorescent dye, 3,3′-dihexyloxacarbocyanine iodide (DiOC$_6$(3)), which accumulates in mitochondria of living cells. MMP hyperpolarization was observed after 1 hr of treatment with either Bz-423 or oligomycin (Figure 4A). In contrast, antimycin A, which inhibits complex III [27], or betulinic acid, which binds to the mitochondrial PT pore [28], did not increase the MMP. To examine the effect of Bz-423

on mitochondrial ATP synthesis, digitonin-permeabilized Ramos cells were treated with Bz-423 and the rate of ATP synthesis was measured [29]. Bz-423 inhibited ATP synthesis in a concentration-dependent manner with an IC$_{50}$ similar to the EC$_{50}$ for apoptosis in these cells (ca. 5 μM [8]; Figure 4B).

In coupled, actively respiring mitochondria (i.e., state 3, ADP present), F_1F_0-ATPase inhibitors induce a transition back to resting levels of respiration (known as state 4) [10]. The critical signal orchestrating apoptosis in response to Bz-423 is O$_2^-$. Our data indicate that this O$_2^-$ results from a state 3 to 4 transition produced as a result of Bz-423 inhibiting the F_1F_0-ATPase. To test this hypothesis directly, digitonin-permeabilized Ramos cells were treated with malate/glutamate as energy sources along with ADP [30], and the rate of O$_2$ consumption was monitored as a function of [Bz-423]. After
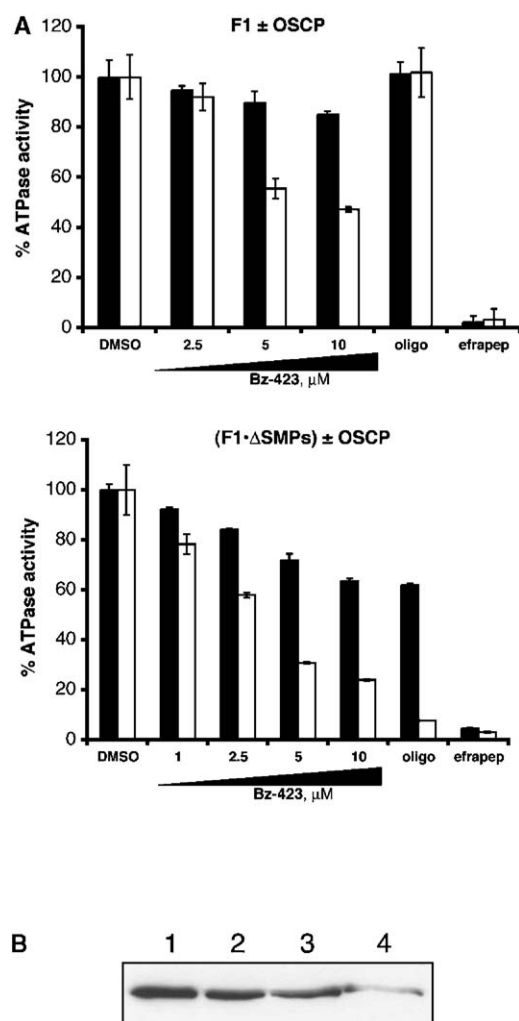
Figure 3. Bz-423 Binds the OSCP

(A) Effect of Bz-423 on F_1 (top) and $F_1 \cdot \Delta SMPs$ (bottom) in the presence (open bars) and absence (filled bars) of the OSCP. Contrast the inhibitory pattern of Bz-423 with the F_1 inhibitor, efrapeptin (efrapep; 1 μM), that inhibited all preparations, and the F_0 binding inhibitor, oligomycin (oligo; 0.1 μM), that required both the OSCP and $\Delta SMPs$ for inhibition. The ATP hydrolysis activity of isolated F_1 was ca. 10 $\mu mol/min/mg$ protein (in the absence of inhibitors).

(B) Western blot analysis of OSCP levels at each step of ΔSMP preparation. Lane 1, starting SMPs; lane 2, SMPs lacking IF1; lane 3, SMPs lacking IF1 & F_1; lane 4, SMPs lacking IF1, F_1, and OSCP ($\Delta SMPs$). GAPDH was used as a protein loading control.

Error bars represent the standard deviation from at least three separate determinations.

the addition of 0.045 $\mu moles$ of Bz-423, the rate of O_2 consumption began to decrease significantly (from 18.5 to 14.8 nmol $O_2/min/30 \times 10^6$ cells; Figure 4C). To ensure this change did not merely result from depletion of the ADP supply, more ADP (200 μmol) was added; the rate did not increase, confirming the presence of sufficient [ADP]. Addition of more Bz-423 continued to decrease the rate of O_2 consumption, until the rate decreased to that observed under state 4 conditions after 0.090 $\mu moles$ total of drug was added. Collectively, this set of studies demonstrates that, in cells, Bz-423 inhib-

its the F_1F_0-ATPase, and as shown below, this activity mediates its proapoptotic effects.

The OSCP couples proton translocation in F_0 to catalysis in F_1 and is therefore required for mitochondrial ATP synthesis [31, 32]. Not surprisingly, yeast OSCP knockouts fail to survive under normal growth conditions [33]. Thus, we expected that knocking out the OSCP in mammalian cells would similarly be lethal. To demonstrate that the OSCP mediates Bz-423-induced apoptosis, the relationship between levels of OSCP and sensitivity to Bz-423 was investigated using RNA interference (RNAi) [34]. Decreasing drug target levels can either sensitize or protect against death by target-specific agents. If target binding by a drug interferes with the ability of that target to provide a growth/survival signal or critical metabolite, then decreasing the level of target will *sensitize* cells to death induced by the agent. This occurs because a constant amount of inhibitor more completely saturates and more completely inhibits the function of the smaller number of target sites available for drug binding (e.g., inhibition of thymidylate synthase [35]). However, if target binding by a drug instead causes the target to generate increased levels of a death-inducing signal, decreasing the level of target will *protect* cells against death induced by that agent because a given drug will not generate as much of the death signal (small molecules that bind to the X-linked inhibitor of apoptosis (XIAP) are example of this mode action [36]). Since Bz-423 initiates cell death by generating O_2^-, we predicted that, at a given [Bz-423], cells with less OSCP would produce less O_2^- (the death signal) and would consequently be protected from Bz-423-induced cell death. Only with a very significant OSCP reduction (i.e., to levels close to knockout) would we predict cells to be more sensitive to Bz-423, as the remaining functional F_1F_0-ATPases would not be able to provide enough ATP for normal cellular function in the presence of Bz-423.

To test this hypothesis, 293 cells were transiently transfected with siRNAs against the OSCP or with a control sequence not in the human genome. OSCP expression was analyzed by immunoblotting at 24, 48, 72, and 96 hr after transfection. Maximum OSCP reduction was observed at 72 hr (Figure 4D, inset; siRNA **2**); therefore, cells were treated with Bz-423 beginning 72 hr after transfection. Consistent with our hypothesis, cells with less OSCP were less sensitive to Bz-423-induced apoptosis than control cells (Figure 4D). The sensitivity of the transfectants to Bz-423-induced apoptosis correlated with the amount of OSCP remaining; OSCP levels in cells transfected with siRNAs **1** and **2** were 55% and 35% of that in control cells, and when treated with 10 μM Bz-423 the transfectants had 64% and 44% the death of the controls, respectively.

Because OSCP levels recover 96 hr following transient transfection, stably transfected 293 cells with reduced OSCP levels ($\delta OSCP$, clones **1** and **2**) were generated for further analysis (Figure 5A). Since mammalian cells with reduced OSCP expression have not been reported, we first characterized the properties of the mitochondria in the $\delta OSCP$ clones. Reducing OSCP levels did not alter expression of the MRC enzymes (data not shown) or other F_1F_0-ATPase subunits (Figure 5A) and had no effect on mitochondrial ultrastructure
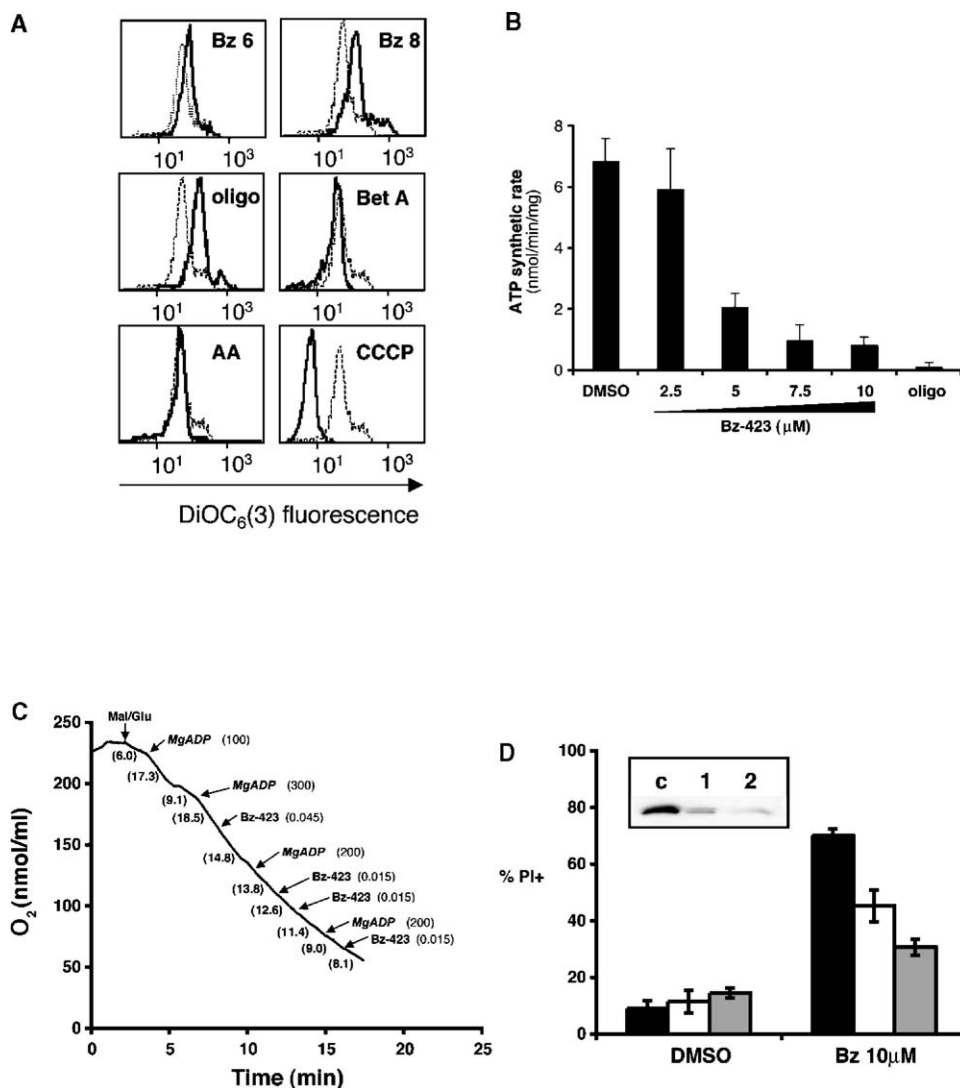
Figure 4. Bz-423 Inhibits the F_1F_0-ATPase in Cells and Induces Cell Death via OSCP Binding

(A) Analysis of MMP in Ramos cells. Cells were treated with Bz-423 (Bz; μM), oligomycin (oligo; 1 μM), betulinic acid (Bet A; 20 μM), antimycin A (AA; 10 μM), or the protonophore, CCCP (50 μM), that abolishes the MMP, for 1 hr, and stained with $DiOC_6$(3). The fluorescence intensity in vehicle control (dashed lines) and treated cells (solid lines) was measured by flow cytometry.

(B) Rate of ATP synthesis in Ramos cells. Cells were permeabilized with digitonin, ADP and malate/glutamate substrates were added, and cells were then treated with Bz-423 or oligomycin (oligo; 0.1 μM). The rate of ATP synthesis was measured using a luciferase-luciferin reporter assay, and ΔRLU was converted to Δ[ATP] using an ATP standard curve. RLU values were corrected for the small amount of luciferase inhibition observed with Bz-423; oligomycin does not affect luciferase activity.

(C) O_2 consumption in Ramos cells. Cells (30 × 10^6) were permeabilized with digitonin, placed in a sealed chamber, malate/glutamate (5 mM) and ADP (μmol) substrates were added as indicated, and the effect of Bz-423 on the rate of oxygen consumption was monitored. Rates (nmol O_2/min/30 × 10^6 cells) are indicated in parentheses under the trace. EtOH alone (1% final concentration) does not inhibit O_2 consumption. The total amount of Bz-423 used in this experiment corresponds to 0.003 μmoles/10^6 cells/ml, which are typical conditions under which the proapoptotic effects of Bz-423 are observed. The rate of O_2 consumption in Ramos cells prevented the use of fewer cells in the assay.

(D) PI permeability (cell death) of 293 cells transiently transfected with 21 bp long siRNAs specific for the OSCP or control sequence and treated with vehicle control or Bz-423: control (black bars), siRNA 1 (white), and siRNA 2 (gray). Inset shows Western blot analysis of OSCP levels in transient transfectants: control (c), siRNA 1 (1; 45% decrease in OSCP), and siRNA 2 (2; 65% decrease). β-tubulin was used as a protein-loading control.

Error bars represent the standard deviation from at least three separate determinations.

(Figure 5B). These latter findings are important since certain genetic changes that affect the F_1F_0-ATPase can drastically alter mitochondrial structure and function [37].

The impact of reducing OSCP levels on the MMP and number of mitochondria was evaluated using confocal microscopy analysis of cells stained with $DiOC_6$(3), which provides an estimate of MMP, and MitoTracker Red 580, which stains mitochondria independent of MMP. MitoTracker Red and $DiOC_6$(3) staining coloca-
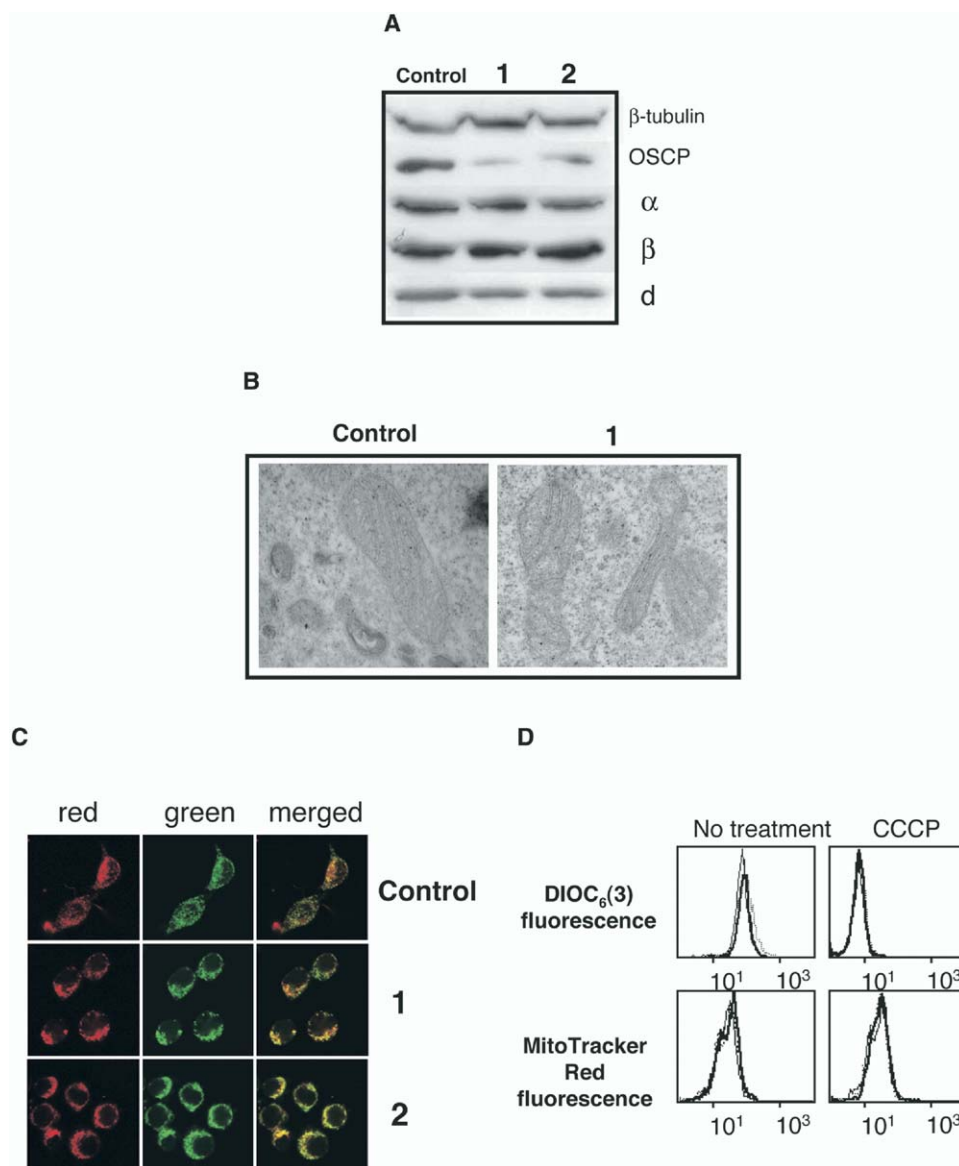
Figure 5. Mitochondrial Analysis of Stably Transfected δOSCP Clones

(A) Western blot of F_1F_0-ATPase subunits in clones 1 (70% OSCP reduction) and 2 (40% OSCP reduction). The mitochondrial levels of other F_1F_0-ATPase subunits (α, β, d) did not change. β-tubulin was used as a protein-loading control.

(B) Electron micrographs of mitochondria in control transfectants (left) and clone 1 (right) (19,600× magnification).

(C) Qualitative analysis of the MMP and number of mitochondria in the clones. Control cells (top) and clones 1 (middle) and 2 (bottom) were coloaded with MitoTracker Red 580 (red stains; mitochondria independent of MMP) and $DiOC_6(3)$ (green; MMP-dependent staining), and images were obtained using fluorescent confocal microscopy. The MitoTracker Red and $DiOC_6(3)$ staining colocalized in all cells, and was indistinguishable between the clones and controls. Each image is representative of three separate experiments.

(D) Quantitative analysis of mitochondria in the clones. Cells were stained with $DiOC_6(3)$ and MitoTracker Red, and the mean fluorescence intensity was measured by flow cytometry. δOSCP clones 1 (thick solid line) and 2 (thin solid line) had very similar MMPs and an indistinguishable number of mitochondria versus control cells (dashed line). CCCP (50 μM) treatment demonstrates that $DiOC_6(3)$ fluorescence is MMP-dependent, while MitoTracker Red fluorescence remains regardless of MMP. The GFP signal in the transfectants is >20-fold weaker than the $DiOC_6(3)$ staining and did not interfere with analysis here or in (C).

lized in the δOSCP clones, and the fluorescence of control cells and δOSCP clones was indistinguishable (Figure 5C). Quantitative analysis by flow cytometry demonstrated that the mean fluorescence intensity of both MitoTracker Red and $DiOC_6(3)$ was nearly identical in the δOSCP clones and control cells (Figure 5D), consistent with the imaging data. Since these experiments demonstrate that reducing OSCP expression does not significantly affect the structure, membrane potential, or number of mitochondria, any differences in the responses of the δOSCP clones to Bz-423 compared to control cells should be directly attributable to the reduced OSCP levels.

Both δOSCP clones were less sensitive to Bz-423

than control cells, and like the transient transfectants, their levels of OSCP expression correlated with their sensitivity to Bz-423 (Figure 6A). Specifically, the OSCP level in clones **1** and **2** was 30% and 60% of that in control cells, and when treated with 11 μM Bz-423 (near the EC_{50} for the control cells), the clones had 39% and 84% the death of controls. In contrast, decreasing OSCP expression did not affect sensitivity to a range of other cytotoxic drugs, including the DNA damaging agents, *cis*-diaminodichloroplatinum (CDDP) and etoposide; the kinase inhibitor, staurosporine; the MRC poisons, antimycin A and *N*-(4-hydroxyphenyl)retinamide (4-HPR); and betulinic acid, which directly triggers the PT pore (Figure 6A). These results show that decreasing OSCP expression specifically attenuates the cytotoxic response to Bz-423.

To determine if the mechanism of cell death in the δOSCP clones changed relative to control cells, the mediators of Bz-423-induced apoptosis were examined. The δOSCP clones generated O_2^- (Figure 6B) and engaged the same downstream death pathways over the same time course as controls (e.g., collapse of the MMP, cytochrome *c* release, caspase activation; data not shown), despite requiring higher [Bz-423] to produce equivalent responses. At a given [Bz-423], O_2^- production in each clone correlated with its OSCP level; clone **2** had more OSCP and generated more O_2^- than clone **1**, while control cells had the highest levels of OSCP and the largest O_2^- response (Figure 6B). In accordance with this observation, the degree of inhibition of state 3 respiration at a given [Bz-423] also correlated with the level of OSCP and O_2^- response (data not shown). When cell death was plotted versus O_2^- as a function of [Bz-423], the curves for the control and clone **1** had similar shapes (Figure 6C), suggesting that the O_2^- response was equally as important for initiating apoptosis in the clones as controls. Moreover, in both the clones and controls, the percentage of cells staining O_2^- positive at 1 hr predicted the level of cell death at 24 hr across a range of [Bz-423]. For example, when treated with 11 μM Bz-423, the percentage of O_2^- positive controls and clones **1** and **2** was 57, 20, and 47%, respectively. After 24 hr, the percentage of dead cells was 57, 22, and 48%. Additionally, the antioxidants, vitamin E and MnTBAP, blocked Bz-423-induced O_2^- and apoptosis as effectively in δOSCP clones as in controls (Figure 6C). These results argue that OSCP expression determines the initial response to Bz-423 (i.e., O_2^- generation) and the clones use the same apoptotic pathway as controls.

Since the O_2^- produced as a result of F_1F_0-ATPase inhibition is the critical signal initiating apoptosis, these data also provide strong evidence that the OSCP, and not another target, is responsible for mediating Bz-423 cell killing. Taken together, these studies demonstrate that the OSCP is the molecular target of Bz-423, and inhibition of the F_1F_0-ATPase is the critical event that initiates O_2^- production and the subsequent apoptotic cascade.

Discussion

1,4-benzodiazepines like diazepam are best known for their action on the central nervous system [38]. At concentrations above those needed for anxiolytic effects, some benzodiazepines also affect cell survival and growth [17]. The mechanism and target responsible for these other activities remains obscure. Early studies suggested that binding to the PBR, an 18 kDa transmembrane protein that forms part of the mitochondrial PT pore, mediated these effects [39]. Yet more recent work has provided cogent evidence against this hypothesis [40]. While Bz-423 binds weakly to the PBR, it is unlikely that this interaction signals apoptosis since Bz-423 is cytotoxic to cells reported to lack the PBR [9], and compounds with much higher affinity for the PBR (e.g., PK11195 and diazepam [17]) do not possess the activity of Bz-423. These observations, along with the selectivity of Bz-423 in vivo, suggested that this benzodiazepine had a novel cellular target.

In contrast to other F_1F_0-ATPase inhibitors, which bind in either F_0 (i.e., oligomycin [18]) or F_1 (i.e., efrapeptin [41] and aurovertin [42]), the Bz-423 inhibitor binds within the peripheral stalk of the enzyme, remote from the active site. It is likely that Bz-423 functions by inducing/blocking a conformational change required for substrate binding and catalysis as reflected by the change in K_m and V_{max} (e.g., see Figure 2B). To validate the OSCP as the target within cells that mediates Bz-423-induced apoptosis, we employed RNAi to generate cells with reduced OSCP levels. As OSCP knockdowns in mammalian cells have not previously been reported, we did not know a priori whether cells with reduced OSCP levels would have significantly altered mitochondrial function and physiology, which would render them an unsuitable cellular model for target validation. However, several lines of evidence suggested that it would be possible to specifically reduce OSCP levels without significantly altering mitochondrial structure, function, or cellular viability.

First, the OSCP is not needed for mammalian F_1 to bind F_0 [32], which predicted that F_1F_0-ATPase subunits would be expressed and assemble properly with or without the OSCP. Second, the MMP is derived from several sources, including activity of the MRC enzymes and proton conduction through F_0. However, expression of MRC complexes and passive proton conduction through F_0 do not require the presence of the OSCP [32], which predicted that OSCP reduction should not significantly alter the MMP. Last, the mitochondrial machinery required for oxidative phosphorylation is present in "biochemical excess" [43, 44]. This means that the oxidative phosphorylation system can compensate for a defect in one component by upregulating other parts of the system; it is only after the defect bypasses a critical threshold that a change in respiration or viability becomes apparent. For example, the F_1F_0-ATPase from rat heart must be inhibited >80% before an effect on respiration can be measured [45].

Based on these considerations, our data indicate that, in the δOSCP clones, F_1F_0-ATPase complexes (± OSCP) and MRC enzymes are expressed and assembled properly. All F_1F_0-ATPase complexes allow dissipation of the proton gradient produced by the MRC, which prevents the MMP from becoming hyperpolarized. Only the F_1F_0-ATPases that have the OSCP are capable of synthesizing ATP that the cells need to survive, but the clones compensate for the fact that they have fewer complexes with OSCP by upregulating the
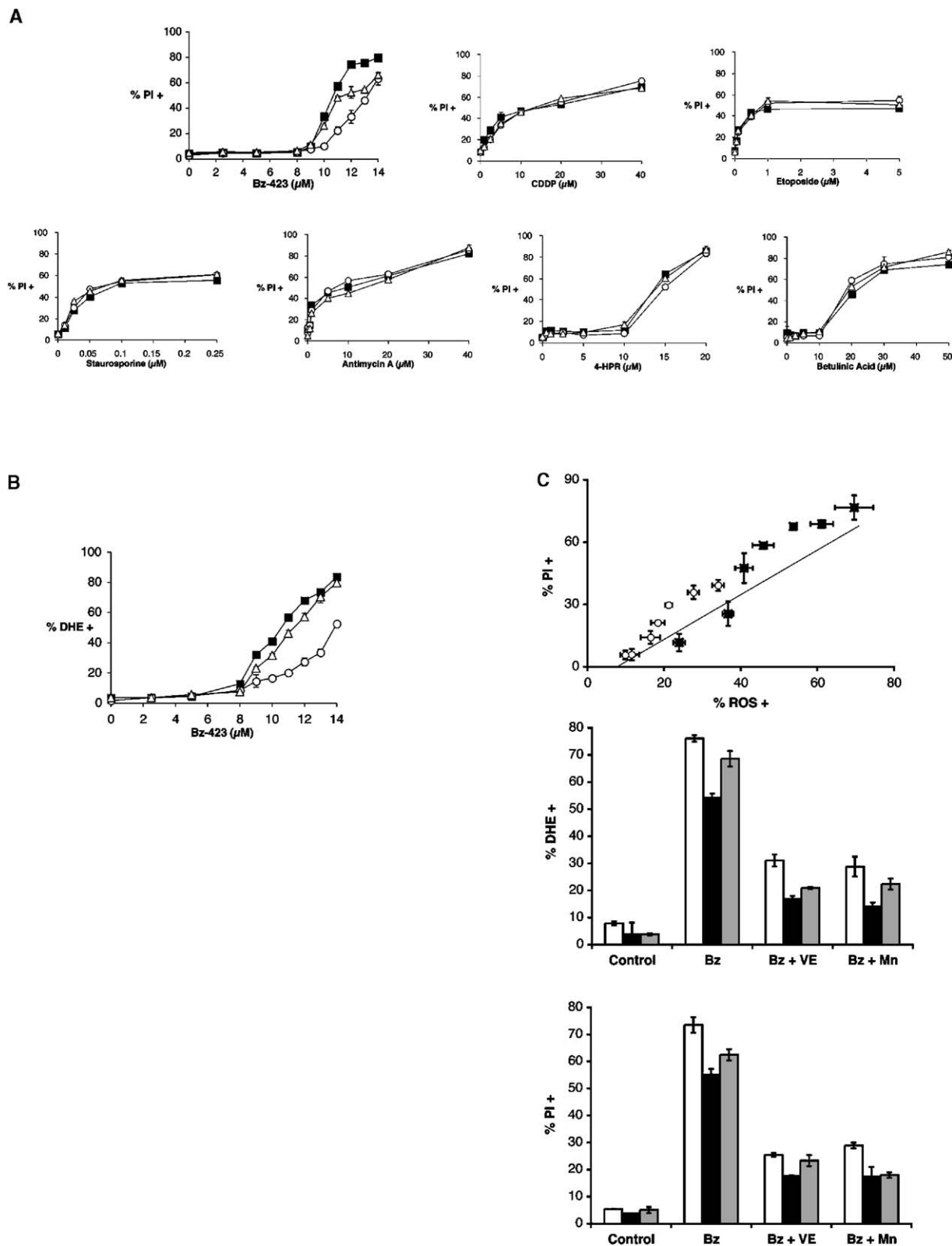
A

B

C

Figure 6. Mechanism of Bz-423-Induced Cell Death in δOSCP Clones

(A) Killing of control cells (closed squares) and clones 1 (open circles) and 2 (open triangles) by Bz-423 and other cytotoxic drugs as measured by PI permeability.

(B) Bz-423 produces a dose-dependent increase in O_2^- in control cells (closed squares) and clones 1 (open squares) and 2 (open triangles).

(C) Dependence of apoptosis on O_2^- in control cells and δOSCP clones. DHE fluorescence was measured at 1 hr and PI permeability at 24 hr. Top: plot of cell death versus O_2^- as a function of increasing [Bz-423] (9–12 μM) for control cells (closed squares) and clone 1 (open circles). Middle/bottom: After preincubation with vitamin E (VE; 100 μM) or MnTBAP (Mn; 100 μM), Bz-423 (15 μM) was added to the cultures; DHE fluorescence was measured at 1 hr (middle) and PI permeability at 24 hr (bottom): control cells (white bars), clones 1 (black bars) and 2 (gray bars).

Error bars represent the standard deviation from at least three separate determinations.

activity of the MRC (unpublished data). These conclusions explain why the δOSCP clones have similar numbers of mitochondria, MMPs, levels of other F_1F_0-ATPase subunits, and mitochondrial ultrastructures as the control cells.

Many inhibitors of the F_1F_0-ATPase, like oligomycin, are natural products, very potent, and extremely toxic [46]. For example, the LD_{33} for oligomycin in rats is 0.5 mg/kg [47]. Although cells treated with oligomycin generate ROS as a result of a state 3 to 4 transition like Bz-423, they also become depleted of ATP and die via necrosis, as apoptosis can only occur with sufficient ATP reserves [48]. In contrast, Bz-423-treated mice show no adverse toxicities [8, 9], and when cells are cultured with Bz-423, they exhibit a limited drop in ATP (see Figure 4B) and die via apoptosis. For Bz-423, it is the O_2^- generated as a result of the state 3 to 4 transition that is the critical signal for initiating cell death. Thus, inhibition of the F_1F_0-ATPase with Bz-423 compared to oligomycin has distinct functional consequences that likely result from differences in the mechanisms of inhibition. Preliminary analysis of the inhibition kinetics (see Figure 2B) suggests that these differences may arise due to disparities in the enzyme-substrate complexes each compound binds to during the stages of the catalytic cycle (unpublished data).

A unique property of Bz-423 is its selective cytotoxicity against activated, autoimmune lymphocytes in vivo [8, 9]. Integrating knowledge of the target of Bz-423 with the properties of autoreactive lymphocytes provides a starting point to explain aspects of this selectivity. For example, lupus lymphocytes have been shown to have 50% more mitochondria than normal immune cells [12], and these mitochondria have lower [ATP], elevated ROS, less glutathione (GSH), and are hyperpolarized compared to normal mitochondria [13, 14]. The exact cause of these abnormalities is not yet clear, although several lines of evidence suggest that they stem from metabolic stress, which is a consequence of the increased energy demand imposed by persistent lymphocyte hyperactivation (a characteristic of human and murine lupus), along with possible defects in the F_1F_0-ATPase itself [13, 14]. Both metabolic stress and F_1F_0-ATPase defects lead to hyperpolarization of $\Delta\psi_m$, and when $\Delta\psi_m$ values rise to >140 mV, excess O_2^- is generated by the MRC [43] and GSH is consumed. Thus, the combination of having more mitochondria (with OSCP target), along with altered mitochondrial bioenergetics, $\Delta\psi_m$, and redox balance, should specifically render lupus lymphocytes sensitive to Bz-423-induced apoptosis. Consistent with this line of reasoning, experimentally reducing levels of GSH sensitizes cells to Bz-423 (unpublished data).

Previous work has demonstrated that pathways of B cell receptor (BCR)-mediated lymphocyte activation interact with Bz-423-induced signals to produce a synergistic death response [26], which may also help to explain why hyperactivated lupus lymphocytes are particularly sensitive to Bz-423. Although the specific point of intersection of these pathways is still being elucidated, calcium is an essential component of the response [26]. Mitochondria play a central role in modulating intracellular Ca^{2+} fluxes, and Ca^{2+} can both stimulate mitochondrial metabolism and ATP production, as well as exert control over mitochondrial apoptosis through the PT pore [49, 50]. The magnitude and duration of Ca^{2+} signals are particularly important for determining the net effect a given signal will have on the mitochondria. A transient Ca^{2+} spike serves primarily to increase metabolism. In contrast, a sustained Ca^{2+} response of greater magnitude and duration is thought to play a greater role in PT induction [50, 51]. While the exact amount of Ca^{2+} uptake needed to induce the MPT is unknown, the amount of Ca^{2+} required is much lower when mitochondrial levels of pyrophosphate and ROS are increased [52]. Thus, the exposure of hyperactivated lupus lymphocytes to Bz-423-induced mitochondrial ROS may be sufficient to convert signals that are normally stimulatory for these pathogenic cells (i.e., Ca^{2+} flux) into death-inducing messengers.

Significance

Bz-423 is a cytotoxic 1,4-benzodiazepine that suppresses autoimmunity and prolongs survival in murine models of lupus by selectively killing disease-causing lymphocytes. Unlike drugs currently used to treat lupus, like cyclophosphamide, Bz-423 blunts autoimmune disease without adverse toxicity or attenuation of normal immune function. Here, using phage display screening, we demonstrated that Bz-423 binds to the OSCP component of the mitochondrial F_1F_0-ATPase and validated that this target mediates Bz-423-induced apoptosis. The Bz-423 inhibitor binds within the peripheral stalk of the F_1F_0-ATPase and compared to compounds like oligomycin, efrapeptin, and aurovertin, which are highly toxic, has a unique mechanism of action. Rather than significantly depleting ATP, inhibition of the F_1F_0-ATPase by Bz-423 leads to a state 3 to 4 transition within mitochondria, resulting in production of O_2^- from the respiratory chain, which is the key signal for apoptosis initiation. Interestingly, lupus lymphocytes have greater numbers of mitochondria, and these mitochondria have elevated ROS, reduced antioxidant stores, and are hyperpolarized compared to normal mitochondria. These alterations likely sensitize autoimmune lymphocytes to Bz-423-induced apoptosis and provide a significant basis for the selectivity observed in vivo. New therapies specifically for the treatment of lupus have not been approved in over 30 years. Our data point to a drug target and mechanism on which to base the development of selective cytotoxic agents with therapeutic potential for lupus and related autoimmune diseases. Given the efficacy and favorable toxicity profile of Bz-423, molecules with similar properties are expected to be promising leads.

Experimental Procedures

Reagents
Bz-423 was synthesized as previously described [53]. DHE, $DiOC_6(3)$, MitoTracker Red 580, and anti-F_1F_0-ATPase antibodies (α, β, d) were from Molecular Probes (Eugene, Oregon). MnTBAP was from Alexis Biochemicals (San Diego, California). ADP and AMP were from Calbiochem (San Diego, California). ATP, NADH,

NADP^{+}, and coupling enzymes were from Roche Applied Science (Indianapolis, Indiana).

Cell Lines and Culture

Human embryonic kidney 293 cells (293 cells) were maintained in DMEM and Ramos B cells were maintained in RPMI; both were supplemented with 10% heat-inactivated FBS, penicillin (100 U/ml), streptomycin (100 μg/ml), and L-glutamine (290 μg/ml). Studies with drugs and inhibitors were performed as previously described [8].

Analysis of Cell Death and O_2^-

Cell viability was measured by propidium iodide (PI) exclusion and O_2^- was measured using DHE by flow cytometry as previously described [8].

Library Screening

A human breast cancer T7 cDNA phage display library (Novagen, San Diego, California) was generated and screened using biotinylated-Bz-423 as previously described [15]. In brief, the library was titered, and 3.7×10^8 plaque forming units (pfu) of phage were suspended in Tris (50 mM), NaCl (0.9 M), and 0.1% Tween (TBST, 500 μl) and combined with avidin beads (200 μl, Pierce, Rockford, Illinois) for 1 hr to remove avidin binding phage. The supernatant was added to fresh beads (200 μl) containing biotinylated Bz-423 (1 ml, 400 μM) in PBS and agitated overnight at 4°C. The beads were collected and washed and the phage was eluted. Eluted phage were amplified and 10^8–10^9 phage particles were used in each subsequent round of selection. After the first round, the incubation time was reduced to 1 hr.

Preparation of Submitochondrial Particles

Mitochondria were isolated from bovine hearts [54] with 2-mercaptoethanol (5 mM) in all buffers, and submitochondrial particles (SMPs) for ATP hydrolysis [19] and synthesis [55] assays were prepared by sonication.

F_1F_0-ATPase Activity

ATP hydrolysis was measured in bovine SMPs by coupling the production of ADP to the oxidation of NADH [56]. ATP synthesis was measured by coupling the production of ATP to the reduction of NADP^{+} [57].

Reconstitution Studies

Bovine heart F_1-ATPase was isolated as described by Walker et al. [19]. The OSCP was expressed and purified as previously described [21, 58]. F_1-ATPase was reconstituted with recombinant bovine OSCP as described by Collinson et al. [21] and the complex was isolated by gel filtration. Bovine heart SMPs were prepared at pH 8.6 with EDTA (2 mM), and were then sequentially depleted of IF1, F_1, and OSCP, yielding ΔSMPs [20]. Aliquots of SMPs from each depletion step were immunoblotted for IF1, β, and OSCP to confirm the removal of the appropriate subunits at each step. ΔSMPs were reconstituted with F_1 alone or F_1 and OSCP [20].

ATP Synthesis and Oxygen Consumption in Whole Cells

Ramos B cells were permeabilized with digitonin (14 μg/10^6 cells; 1×10^7 cells/ml; 3 min), and the rates of mitochondrial ATP synthesis and oxygen consumption were measured in the presence of malate/glutamate substrates as previously described [29, 30], with the exception that bovine serum albumin was excluded from the measurement buffer. For ATP synthesis, the luciferase-luciferin assay was monitored continuously over 30 min using a 96-well plate-reading luminometer, and synthetic rates were evaluated over a time frame in which the ATP synthetic rate was linear. Relative luminescence units (RLU) were converted to [ATP] using an ATP standard curve. A Hansatech oxygen electrode and Oxygraph software were used for monitoring and analyzing oxygen consumption.

Transfection with Small Interfering RNAs To Reduce OSCP

RNA oligonucleotide duplexes (21 bp long), complimentary to regions within the OSCP mRNA, designated siRNA **1** (AAG CCT AAA TGA CAT CAC AGC) and siRNA **2** (AAG TGT TGG TTT TCT GCC ATC), and a 19 bp long control RNA sequence not present in the

human genome (ACT ACC GTT GTT ATA GGT G) were obtained (Dharmacon; Boulder, Colorado). 293 cells were transfected with the siRNAs (200 nM) using Oligofectamine (Invitrogen; San Diego, California) and screened for OSCP expression by immunoblotting at indicated time points.

Establishing OSCP siRNA Stable Transfectants

A pGEM1 plasmid containing the human U6 gene locus was used as the template to PCR amplify a 350 bp long fragment of the U6 RNA promoter with primer pairs: ACGGTAATACGACTCACTA TAGGG and CTACGTCGACCGACGGCCAGTGCCAAGCTT. This fragment was cloned into pEGFP-N1 (Clontech, San Diego, California) immediately 5′ of the CMV promoter. The resulting construct is designated pEGFP-N1-U6. To reduce OSCP expression, an oligonucleotide containing a 19 bp long inverted repeat (underlined below) complimentary to the human OSCP mRNA, GATTCC<u>GTG TTGGTTTTCTGCCATCTTCAAGAGA</u>GATGGCAGAAAACCAACAC TTTTTTG, was cloned into pEGFP-N1-U6 (designated p-iOSCP). 293 cells were transfected using Oligofectamine with this plasmid or a vector control containing a sequence of identical length not present in the human genome. After transfection (48 hr), cells were sorted by flow cytometry on the basis of GFP fluorescence and individual clones were expanded in the presence of geneticin (G418; 1.5 mg/ml). Of eleven clones, two had significantly reduced OSCP expression as determined by immunoblotting followed by densitometry quantification. Mitochondria were isolated from the clones [55] and immunoblotted for levels of other F_1F_0-ATPase subunits (α, β, d).

Analysis Mitochondria in Stable Transfectants

Cells were grown on chamber slides and loaded with complete medium containing $DiOC_6(3)$ (20 nM) and MitoTracker Red 580 (50 nM) for 30 min at 37°C. Cells were washed with PBS and examined using an MRC-600 laser scanning confocal microscope. For quantitative analysis of mitochondria by flow cytometry, cells were stained as described above, and mean fluorescence intensity was determined. Electron microscopy samples were prepared as previously described [59] and viewed on a Philips CM100 at 60kV.

References

1. Lawrence, R.C., Hochberg, M.C., Kelsey, J.L., McDuffie, F.C., Medsger, T.A., Jr., Felts, W.R., and Shulman, L.E. (1989). Estimates of the prevalence of selected arthritic and musculoskeletal diseases in the United States. J. Rheumatol. *16*, 427–441.
2. Shlomchik, M.J., Craft, J.E., and Mamula, M.J. (2001). From T to B and back again: positive feedback in systemic autoimmune disease. Nat. Rev. Immunol. *1*, 147–153.
3. Oates, J.C., and Gilkeson, G.S. (2002). Mediators of injury in lupus nephritis. Curr. Opin. Rheumatol. *14*, 498–503.
4. Baechler, E.C., Batliwalla, F.M., Karypis, G., Gaffney, P.M., Ortmann, W.A., Espe, K.J., Shark, K.B., Grande, W.J., Hughes, K.M., Kapur, V., et al. (2003). Interferon-inducible gene expression signature in peripheral blood cells of patients with severe lupus. Proc. Natl. Acad. Sci. USA *100*, 2610–2615.
5. Gescuk, B.D., and Davis, J.C., Jr. (2002). Novel therapeutic agents for systemic lupus erythematosus. Curr. Opin. Rheumatol. *14*, 515–521.
6. Petri, M. (2004). Cyclophosphamide: new approaches for systemic lupus erythematosus. Lupus *13*, 366–371.

7. Schreiber, S.L. (2000). Target-oriented and diversity-oriented organic synthesis in drug discovery. Science *287*, 1964–1969.

8. Blatt, N.B., Bednarski, J.J., Warner, R.E., Leonetti, F., Johnson, K.M., Boitano, A., Yung, R., Richardson, B.C., Johnson, K.J., Ellman, J.A., et al. (2002). Benzodiazepine-induced superoxide signals B cell apoptosis: mechanistic insight and potential therapeutic utility. J. Clin. Invest. *110*, 1123–1132.

9. Bednarski, J.J., Warner, R.E., Rao, T., Leonetti, F., Yung, R., Richardson, B.C., Johnson, K.J., Ellman, J.A., Opipari, A.W., Jr., and Glick, G.D. (2003). Attenuation of autoimmune disease in Fas-deficient mice by treatment with a cytotoxic benzodiazepine. Arthritis Rheum. *48*, 757–766.

10. Korshunov, S.S., Skulachev, V.P., and Starkov, A.A. (1997). High protonic potential actuates a mechanism of production of reactive oxygen species in mitochondria. FEBS Lett. *416*, 15–18.

11. Devenish, R.J., Prescott, M., Boyle, G.M., and Nagley, P. (2000). The oligomycin axis of mitochondrial ATP synthase: OSCP and the proton channel. J. Bioenerg. Biomembr. *32*, 507–515.

12. Nagy, G., Barcza, M., Gonchoroff, N., Phillips, P.E., and Perl, A. (2004). Nitric oxide-dependent mitochondrial biogenesis generates Ca2+ signaling profile of lupus T cells. J. Immunol. *173*, 3676–3683.

13. Kuhnke, A., Burmester, G.R., Krauss, S., and Buttgereit, F. (2003). Bioenergetics of immune cells to assess rheumatic disease activity and efficacy of glucocorticoid treatment. Ann. Rheum. Dis. *62*, 133–139.

14. Perl, A., Gergely, P., Jr., Nagy, G., Koncz, A., and Banki, K. (2004). Mitochondrial hyperpolarization: a checkpoint of T-cell life, death and autoimmunity. Trends Immunol. *25*, 360–367.

15. Sche, P.P., McKenzie, K.M., White, J.D., and Austin, D.J. (1999). Display cloning: functional identification of natural product receptors using cDNA-phage display. Chem. Biol. *6*, 707–716.

16. Boyer, P.D. (1997). The ATP synthase–a splendid molecular machine. Annu. Rev. Biochem. *66*, 717–749.

17. Beurdeley-Thomas, A., Miccoli, L., Oudard, S., Dutrillaux, B., and Poupon, M.F. (2000). The peripheral benzodiazepine receptors: a review. J. Neurooncol. *46*, 45–56.

18. Nagley, P., Hall, R.M., and Ooi, B.G. (1986). Amino acid substitutions in mitochondrial ATPase subunit 9 of Saccharomyces cerevisiae leading to oligomycin or venturicidin resistance. FEBS Lett. *195*, 159–163.

19. Walker, J.E., Collinson, I.R., Van Raaij, M.J., and Runswick, M.J. (1995). Structural analysis of ATP synthase from bovine heart mitochondria. Methods Enzymol. *260*, 163–190.

20. Ernster, L., Hundal, T., and Sandri, G. (1986). Resolution and reconstitution of F0F1-ATPase in beef heart submitochondrial particles. Methods Enzymol. *126*, 428–433.

21. Collinson, I.R., van Raaij, M.J., Runswick, M.J., Fearnley, I.M., Skehel, J.M., Orriss, G.L., Miroux, B., and Walker, J.E. (1994). ATP synthase from bovine heart mitochondria. In vitro assembly of a stalk complex in the presence of F1-ATPase and in its absence. J. Mol. Biol. *242*, 408–421.

22. Dupuis, A., and Vignais, P.V. (1987). Interaction between the oligomycin sensitivity conferring protein and the F0 sector of the mitochondrial adenosinetriphosphatase complex: cooperative effect of the F1 sector. Biochemistry *26*, 410–418.

23. Penefsky, H.S., and Cross, R.L. (1991). Structure and mechanism of FoF1-type ATP synthases and ATPases. Adv. Enzymol. Relat. Areas Mol. Biol. *64*, 173–214.

24. Machida, K., and Tanaka, T. (1999). Farnesol-induced generation of reactive oxygen species dependent on mitochondrial transmembrane potential hyperpolarization mediated by F(0)F(1)-ATPase in yeast. FEBS Lett. *462*, 108–112.

25. Gregory, C.D., Tursz, T., Edwards, C.F., Tetaud, C., Talbot, M., Caillou, B., Rickinson, A.B., and Lipinski, M. (1987). Identification of a subset of normal B cells with a Burkitt's lymphoma (BL)-like phenotype. J. Immunol. *139*, 313–318.

26. Bednarski, J.J., Lyssiotis, C.A., Roush, R., Boitano, A.E., Glick, G.D., and Opipari, A.W., Jr. (2004). A novel benzodiazepine increases the sensitivity of B cells to receptor stimulation with synergistic effects on calcium signaling and apoptosis. J. Biol. Chem. *279*, 29615–29621.

27. Matsuno-Yagi, A., and Hatefi, Y. (2001). Ubiquinol:cytochrome c oxidoreductase (complex III). Effect of inhibitors on cyto-

chrome b reduction in submitochondrial particles and the role of ubiquinone in complex III. J. Biol. Chem. *276*, 19006–19011.

28. Fulda, S., Scaffidi, C., Susin, S.A., Krammer, P.H., Kroemer, G., Peter, M.E., and Debatin, K.M. (1998). Activation of mitochondria and release of mitochondrial apoptogenic factors by betulinic acid. J. Biol. Chem. *273*, 33942–33948.

29. Manfredi, G., Spinazzola, A., Checcarelli, N., and Naini, A. (2001). Assay of mitochondrial ATP synthesis in animal cells. Methods Cell Biol. *65*, 133–145.

30. Villani, G., and Attardi, G. (2001). In vivo measurements of respiration control by cytochrome c oxidase and in situ analysis of oxidative phosphorylation. Methods Cell Biol. *65*, 119–131.

31. Mukhopadhyay, A., Zhou, X.Q., Uh, M., and Mueller, D.M. (1992). Heterologous expression, purification, and biochemistry of the oligomycin sensitivity conferring protein (OSCP) from yeast. J. Biol. Chem. *267*, 25690–25696.

32. Pringle, M.J., Kenneally, M.K., and Joshi, S. (1990). ATP synthase complex from bovine heart mitochondria. Passive H+ conduction through F0 does not require oligomycin sensitivity-conferring protein. J. Biol. Chem. *265*, 7632–7637.

33. Prescott, M., Bush, N.C., Nagley, P., and Devenish, R.J. (1994). Properties of yeast cells depleted of the OSCP subunit of mitochondrial ATP synthase by regulated expression of the ATP5 gene. Biochem. Mol. Biol. Int. *34*, 789–799.

34. Lavery, K.S., and King, T.H. (2003). Antisense and RNAi: powerful tools in drug target discovery and validation. Curr. Opin. Drug Discov. Devel. *6*, 561–569.

35. Schmitz, J.C., Chen, T.M., and Chu, E. (2004). Small interfering double-stranded RNAs as therapeutic molecules to restore chemosensitivity to thymidylate synthase inhibitor compounds. Cancer Res. *64*, 1431–1435.

36. Nikolovska-Coleska, Z., Xu, L., Hu, Z., Tomita, Y., Li, P., Roller, P.P., Wang, R., Fang, X., Guo, R., Zhang, M., et al. (2004). Discovery of embelin as a cell-permeable, small-molecular weight inhibitor of XIAP through structure-based computational screening of a traditional herbal medicine three-dimensional structure database. J. Med. Chem. *47*, 2430–2440.

37. Arselin, G., Vaillier, J., Salin, B., Schaeffer, J., Giraud, M.F., Dautant, A., Brethes, D., and Velours, J. (2004). The modulation in subunits e and g amounts of yeast ATP synthase modifies mitochondrial cristae morphology. J. Biol. Chem. *279*, 40392–40399.

38. Whiting, P.J. (2003). The GABAA receptor gene family: new opportunities for drug development. Curr. Opin. Drug Discov. Devel. *6*, 648–657.

39. Wang, J.K., Morgan, J.I., and Spector, S. (1984). Benzodiazepines that bind at peripheral sites inhibit cell proliferation. Proc. Natl. Acad. Sci. USA *81*, 753–756.

40. Gorman, A.M., O'Beirne, G.B., Regan, C.M., and Williams, D.C. (1989). Antiproliferative action of benzodiazepines in cultured brain cells is not mediated through the peripheral-type benzodiazepine acceptor. J. Neurochem. *53*, 849–855.

41. Abrahams, J.P., Buchanan, S.K., Van Raaij, M.J., Fearnley, I.M., Leslie, A.G., and Walker, J.E. (1996). The structure of bovine F1-ATPase complexed with the peptide antibiotic efrapeptin. Proc. Natl. Acad. Sci. USA *93*, 9420–9424.

42. van Raaij, M.J., Abrahams, J.P., Leslie, A.G., and Walker, J.E. (1996). The structure of bovine F1-ATPase complexed with the antibiotic inhibitor aurovertin B. Proc. Natl. Acad. Sci. USA *93*, 6913–6917.

43. Rossignol, R., Faustin, B., Rocher, C., Malgat, M., Mazat, J.P., and Letellier, T. (2003). Mitochondrial threshold effects. Biochem. J. *370*, 751–762.

44. Faustin, B., Rossignol, R., Rocher, C., Benard, G., Malgat, M., and Letellier, T. (2004). Mobilization of adenine nucleotide translocators as molecular bases of the biochemical threshold effect observed in mitochondrial diseases. J. Biol. Chem. *279*, 20411–20421.

45. Rossignol, R., Malgat, M., Mazat, J.P., and Letellier, T. (1999). Threshold effect and tissue specificity. Implication for mitochondrial cytopathies. J. Biol. Chem. *274*, 33426–33432.

46. Wallace, K.B., and Starkov, A.A. (2000). Mitochondrial targets of drug toxicity. Annu. Rev. Pharmacol. Toxicol. *40*, 353–388.

47. Kramar, R., Hohenegger, M., Srour, A.N., and Khanakah, G.

(1984). Oligomycin toxicity in intact rats. Agents Actions *15*, 660–663.

48. Eguchi, Y., Shimizu, S., and Tsujimoto, Y. (1997). Intracellular ATP levels determine cell death fate by apoptosis or necrosis. Cancer Res. *57*, 1835–1840.

49. Rizzuto, R., Pinton, P., Ferrari, D., Chami, M., Szabadkai, G., Magalhaes, P.J., Di Virgilio, F., and Pozzan, T. (2003). Calcium and apoptosis: facts and hypotheses. Oncogene *22*, 8619–8627.

50. Gunter, T.E., Yule, D.I., Gunter, K.K., Eliseev, R.A., and Salter, J.D. (2004). Calcium and mitochondria. FEBS Lett. *567*, 96–102.

51. Gunter, T.E., and Gunter, K.K. (2001). Uptake of calcium by mitochondria: transport and possible function. IUBMB Life *52*, 197–204.

52. Jacobson, J., and Duchen, M.R. (2004). Interplay between mitochondria and cellular calcium signalling. Mol. Cell. Biochem. *256–257*, 209–218.

53. Bunin, B.A., Plunkett, M.J., and Ellman, J.A. (1994). The combinatorial synthesis and chemical and biological evaluation of a 1,4-benzodiazepine library. Proc. Natl. Acad. Sci. USA *91*, 4708–4712.

54. Graham, J.M. (1999). Subcellular fractionation and isolation of organelles: isolation of mitochondria from tissues and cells by differential centrifugation. In Current Protocols in Cell Biology (New York: John Wiley & Sons, Inc.), pp. 3.3.3–3.3.4.

55. Pallotti, F., and Lenaz, G. (2001). Isolation and subfractionation of mitochondria from animal cells and tissue culture lines. Methods Cell Biol. *65*, 1–35.

56. McEnery, M.W., and Pedersen, P.L. (1986). Diethylstilbestrol. A novel F0-directed probe of the mitochondrial proton ATPase. J. Biol. Chem. *261*, 1745–1752.

57. Cross, R.L., and Kohlbrenner, W.E. (1978). The mode of inhibition of oxidative phosphorylation by efrapeptin (A23871). Evidence for an alternating site mechanism for ATP synthesis. J. Biol. Chem. *253*, 4865–4873.

58. Joshi, S., Cao, G.J., Nath, C., and Shah, J. (1996). Oligomycin sensitivity conferring protein of mitochondrial ATP synthase: deletions in the N-terminal end cause defects in interactions with F1, while deletions in the C-terminal end cause defects in interactions with F0. Biochemistry *35*, 12094–12103.

59. Opipari, A.W., Jr., Tan, L., Boitano, A.E., Sorenson, D.R., Aurora, A., and Liu, J.R. (2004). Resveratrol-induced autophagocytosis in ovarian cancer cells. Cancer Res. *64*, 696–703.